Science of the Total Environment 442 (2013) 405–419

Contents lists available at SciVerse ScienceDirect

Science of the Total Environment

journal homepage: www.elsevier.com/locate/scitotenv

Climate change impacts on crop production in Iran's Zayandeh-Rud River Basin

Alireza Gohari [a,c,*,1], Saeid Eslamian [a], Jahangir Abedi-Koupaei [a], Alireza Massah Bavani [b], Dingbao Wang [c], Kaveh Madani [c]

[a] Department of Water Engineering, College of Agriculture, Isfahan University of Technology, Isfahan, Iran
[b] Department of Irrigation and Drainage Engineering, College of Abureyhan, University of Tehran, Iran
[c] Department of Civil, Environmental and Construction Engineering, University of Central Florida, Orlando, FL 32816, USA

HIGHLIGHTS

- Assessment of climate change impacts on crop productivity in central Iran
- Application of ensemble scenarios to deal with uncertainty in climate projections
- Warming shortens the crop growth period.
- Overall crop productivity reduces with lower precipitation and higher temperature.
- Continued production of rice and corn is not recommended under climate change.

GRAPHICAL ABSTRACT

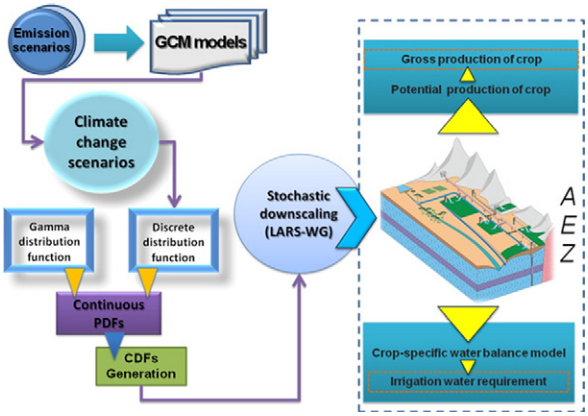

ARTICLE INFO

Article history:
Received 19 June 2012
Received in revised form 19 September 2012
Accepted 5 October 2012
Available online 23 November 2012

Keywords:
Climate change
Agriculture
Crop production
Water resources management
Zayandeh-Rud
Iran

ABSTRACT

This study evaluates climate change impacts on crop production and water productivity of four major crops (wheat, barley, rice, and corn) in Iran's Zayandeh-Rud River Basin. Multi-model ensemble scenarios are used to deal with uncertainties in climate change projections for the study period (2015–2044). On average, monthly temperature will increase by 1.1 to 1.5 °C under climate change. Monthly precipitation changes may be positive or negative in different months of the year. Nevertheless, on the annual basis, precipitation will decrease by 11 to 31% with climate change. While warming can potentially shorten the crop growth period, crop production and water productivity of all crops are expected to decrease due to lower precipitation and higher water requirements under higher temperature. Out of the four studied crops, rice and corn are more vulnerable to climate change due to their high irrigation water demand. So, their continued production can be compromised under climate change. This finding is of particular importance, given the locally high economic and food value of these crops in central Iran.

* Corresponding author at: Department of Water Engineering, College of Agriculture, Isfahan University of Technology, Isfahan, Iran. Tel.: +98 311 391 3432; fax: +98 311 391 2254.
E-mail addresses: Alireza.Gohari@ucf.edu (A. Gohari), saeid@cc.iut.ac.ir (S. Eslamian), koupai@cc.iut.ac.ir (J. Abedi-Koupaei), armassah@ut.ac.ir (A. Massah Bavani), Dingbao.Wang@ucf.edu (D. Wang), Kaveh.Madani@ucf.edu (K. Madani).
[1] Present address: Hydro-Environmental & Energy Systems Analysis (HEESA) Research Group, Department of Civil, Environmental and Construction Engineering, University of Central Florida, Orlando, FL 32816, USA. Tel.: +1 407 823 2317; fax: +1 407 823 3315.

0048-9697/$ – see front matter © 2012 Elsevier B.V. All rights reserved.
http://dx.doi.org/10.1016/j.scitotenv.2012.10.029

1. Introduction

Man-made greenhouse gas emissions as a result of industrialization and urbanization have made significant contributions to global warming and further changes in the global climate. As a result, global temperature rose by 0.74 °C from 1906 to 2005 (IPCC, 2007). Global warming also causes changes in precipitation levels and patterns due to higher evapotranspiration and water vapor amounts in the atmosphere with several implications for the global hydrological cycle (Xu et al., 2006; Zhang et al., 2008, 2010; Eslamian et al., 2012). As the major water consumer of the developing world and some developed countries, agriculture is one of the most vulnerable water sectors to climate change. Dramatic population growth, associated with reduction of productive land area and water resources, exerts extra pressure on the agricultural sector. To ensure sustainability of agriculture, studying the possible climate change impacts on this sector is essential.

Previous studies of climate change impacts on agriculture, using crop yield simulation models such as CERES-maize, CORAC, and EPIC models (Cai et al., 2009a; Mozny et al., 2009; Niu et al., 2009; Chaves et al., 2009; Laux et al., 2010; White et al., 2011), or statistical models (Roudier et al., 2011; Liu et al., 2010; Zhu et al., 2011) suggest that climate change might limit crop production (the amount of a crop that is harvested in a farm, region, state, or country in kilograms or tons) in many areas. Temperature increases affect most plants, leading to crop yield reduction and complex growth responses. Nevertheless, the impact of increasing temperatures can vary widely between crops and regions. For example, a 1 °C increase in the growing period temperature may reduce wheat production by about 3–10% (You et al., 2009); winter wheat productions may be decreased by 5–35%, respectively, under the future warmer and drier conditions (Ozdogan, 2011); and corn yield may be reduced by 2.4–45.6% with higher temperatures (Tao and Zhang, 2010). Even if precipitation is unchanged, the crop production may decrease by 15% on average due to the reduction in crop growth period and increased water stress as the result of higher temperature and evapotranspiration (Schlenker and Lobell, 2010). Expected precipitation reductions in arid and semi-arid regions of the world, where water is already limited, can have dramatic impacts on crop production. For example, in northwestern Turkey, winter wheat yield may decline more than 20% under future climate change because the growth periods can be shortened as a result of increased temperature, exacerbated by a reduction in precipitation (Ozdogan, 2011). In some other areas, climate change might have positive impacts on agricultural crop yield. For example, in dry regions precipitation increases under wet climate warming may lead to improved crop production. Chaves et al. (2009) report that corn, rice, potato, and winter wheat crop production can increase with increasing temperature and precipitation in the North China Plain.

Water demand of most crops is much higher than rainfall in arid and semi-arid regions. Therefore, irrigation is essential to meet the agricultural water demand, in these regions, where a major portion of water withdrawal is allocated to agriculture. In recent years, share of groundwater in the total water used for irrigation has increased in many areas to compensate for the surface water shortages, resulting in serious groundwater depletion, threatening the long-term sustainable agricultural development. In the face of such a threat, developing effective water resources management practices that minimize the negative effects of climate change is necessary.

Effective agricultural water management requires knowledge of crop water requirement, water use efficiency and water productivity (the amount of the physical production of a crop per unit volume of water used), which can be affected by climate change (Mo et al., 2009; Chen and Wang, 2010; Tao and Zhang, in press). As efficiency term, the water productivity expresses the amounts of agricultural outputs in relation to the amount of water needed to produce that output. Water productivity is expressed as the ratio of a mass (kg or ton) and volume of water used (m^3). Higher temperatures can generally increase the irrigation water requirement. While increased irrigation can result in higher crop production even under higher temperatures, generally lower crop production is expected with global warming due to the limited water supply (Chen and Wang, 2010). Climate warming can affect water use efficiency differently. For example, the analysis of climate change effects on the terrestrial ecosystems in China suggests that climate change may have different effects on water use efficiency in farm lands in southern regions, and improved water use efficiency can be seen in forest areas, and high latitude and altitude (Zhu et al., 2011). Quantification of the changes in climate variables such as temperature and precipitation is the first step in climate change impact assessments. The general circulation models (GCMs) are considered as the most credible tools for the projections of future global climate change (IPCC, 2007). Moss and Schneider (2000) discuss that the uncertainty in the GCMs' outputs are mainly due to: (1) the uncertainties in future greenhouse gas and aerosol emissions (related to the emission scenarios) (Parry et al., 2004); (2) the uncertainties in GCMs (Sajjad Khan et al., 2006); and (3) the uncertainties in global climate model sensitivities (Elmahdi et al., 2008). Several methods have been used to manage these uncertainties and to improve our understanding of the physical and biological processes under climate change.

Single GCMs have been traditionally used in climate change impact studies (e.g., Jonesa and Thornton, 2003; Parry et al., 2004; Zhang and Liu, 2005; Zhang and Nearing, 2005; O'Neal et al., 2005; Thomson et al., 2006; Guo et al., 2010; Teixeira et al., in press). However, a single GCM may fail to represent a full range of plausible climate projections, leading to unreliable projections of the future, inappropriate decision-making, and strategy development for adaptation to climate change. Therefore, some climate change studies have used multiple climate change scenarios produced by different GCMs in order to better understand the range of possible climate change impacts and/or develop reliable adaptation strategies (e.g., Medellin-Azuara et al., 2008; Buytaert et al., 2009; Masutomi et al., 2009; Madani and Lund, 2010; Kloster et al., 2010; Connell-Buck et al., 2011; Brian et al., 2011; Lobell and Field, 2011; Lee et al., 2011; Hoglind et al., in press; Guegan et al., 2012; Abrishamchi et al., 2012).

Generally, multi-model projections can be categorized into two groups: equally probable projections and weighted projections (Knutti et al., 2010). In the first category, each component of the ensemble models is assumed to represent an equally probable representation of future climatic conditions (Tao et al., 2009; Lizumi et al., 2009; Tao and Zhang, 2010; Daccache et al., 2011; Ozdogan, 2011). Some studies recommend taking an average over the set of GCMs' outputs to develop a plausible climate change scenario (e.g., Bader et al., 2008; Liu et al., 2010). The second category of multi-model projections include the weighed multi-models that better capture the uncertainty effects (Schmittner et al., 2005; Willby and Harris, 2006; Connolley and Bracegirdle, 2007; Murphy et al., 2007; Waugh and Eyring, 2008). In these multi-models, the models are weighted based on their ability to reproduce the observed climate variables (Greene et al., 2006; Lopez et al., 2006; Furrer et al., 2007; Elmahdi et al., 2008; Cai et al., 2009b).

This paper aims to assess the agricultural responses to climate change in Iran's Zayandeh-Rud River Basin. In particular, the paper estimates the climate change impacts on crop production and water productivity (WP) within a probabilistic multi-model framework. In this framework the uncertainties of GCMs, emission scenarios, and climate variability of daily time series are handled by a downscaling method that combines change factors and a weather generator. The suggested approach tries to improve the reliability of the climate change impact assessment approach by considering the three main sources of uncertainty as discussed earlier. The paper is structured as follows. Section 2 introduces the study area. The selected GCMs and the suggested study method are described in Section 3. Section 4 provides the study results. The limitations of this study have been presented in

Section 5. Section 6 concludes and provides specific recommendations for agriculture water management of the study area.

2. Zayandeh-Rud River Basin

The semi-arid Zayandeh-Rud River Basin is one of the most strategic river basins of Iran (Madani and Marino, 2009). This river basin with an area of 41,347 km^2 is located in central Iran, between the 50° 24′ to 53° 24′ longitudes and 31° 11′ to 33° 42′ latitudes (Fig. 1). The annual precipitation varies from 1500 mm in the west to 50 mm in the east of the basin. The Zayandeh-Rud River, with an average natural flow of 1400 million cubic meters (mcm) per year, including 650 mcm of natural flow and 750 mcm of inter-basin transferred flow, starts in the Zagros Mountains in the west of the basin and ends in the Gav-Khuni Marsh—a preserved marsh under the Ramsar Convention—in the east of the basin. In its west–east journey, Zayandeh-Rud River passes several agricultural and urban areas, including the populous city of Isfahan—the former capital of Iran. This makes the river the most important water resource of the basin for more than 3.7 million residents and their urban, industrial, and agriculture water consumptions, as well as for the survival of the Gav-Khuni Marsh and its valuable ecosystem.

Currently, more than 73% of the basin's available water resources are used for agriculture. Zayandeh-Rud River Basin has 6 irrigation networks, which are located in the lower sub-basins (Abshar, Nekuabad, Rudasht, Mahyar-Jarghuyeh, Borkhar, and Traditional networks). This study focuses on three of them, namely the Abshar, Nekuabad, and Borkhar networks due to their higher importance, senior water rights, high water uses for crop irrigation, and larger cultivated areas. The main traditional staple crops of these networks considered here are wheat, rice, barley, and corn. The other crops cultivated in this basin include potato, alfalfa, tomato, garden production, etc. The areas under cultivation of these crops in the selected irrigation networks are given in Table 1. This study focuses on the three major traditional staple crops of the basin.

3. Method

Fig. 2 indicates the main steps of this study: (1) analyzing monthly temperature and precipitation changes in the study area from 10 GCMs under different climate change scenarios; (2) constructing cumulative probability distributions of different climate change scenarios and estimating changes of climate variables at different probability percentiles; (3) generating daily time series of temperature and precipitation at different probability percentiles by a weather generator, i.e., LARS-WG (Semenov and Barrow, 2002); and (4) studying climate change impacts on crop production and water productivity at different probability percentiles using the Agro-Ecological Zones (AEZ) method (FAO, 1978).

3.1. Generation of climate change scenarios

GCMs are commonly used in climate change impact assessment studies. In this study, the outputs of 10 GCMs under two emission scenarios (A2 and B1) from the Fourth Assessment Report (AR4) of Intergovernmental Panel on Climate Change (IPCC) are used. The detailed description of the selected models is provided in Table 2. The historical meteorological data used in this study belong to the Isfahan Synoptic Station (Fig. 1). A2 and B1 emission scenarios have been commonly used in climate change studies. A2 scenarios assume rapid population growth coupled with slow economic and technological development until 2100. B1 scenarios are characterized by very rapid global socio-economic growth and population rising until 2050 and then declining toward the end of the century. One grid point of each GCM was sufficient to cover the whole study area. The differences of the temperature and relative precipitation in the 30-year monthly average future period (2015–2044) and baseline period (1971–2000) are calculated for each month. In the first step, monthly temperature and precipitation data for the baseline period (1971–2000) and future period (2015–2044) are extracted from the data distribution center of IPCC (DDC: http://www.ipcc-data.org/). In response to the need of the decision

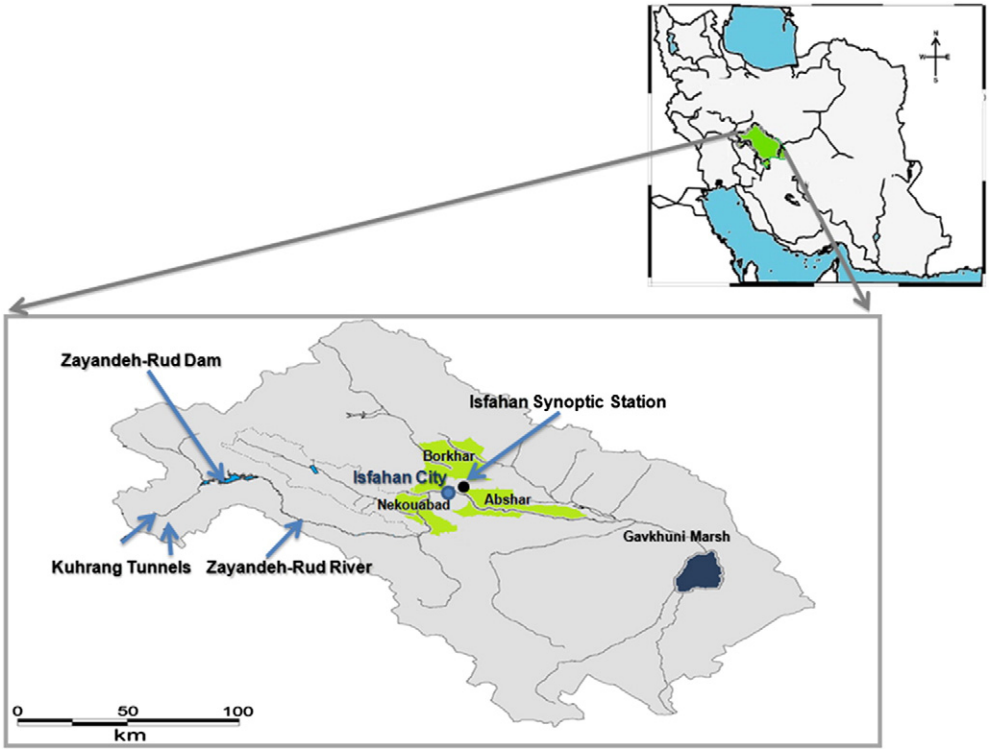

Fig. 1. Zayandeh-Rud River Basin and location of selected irrigation networks.

Table 1
The area under cultivation of major crops in the selected irrigation networks (ha) (Zayandab Consulting Engineering Co., 2008).

Irrigation network	Wheat	Barley	Rice	Corn	Other crops
Abshar	21,496	4024	–	4560	4920
Nekouabad	17,601	7405	14,242	2755	2997
Borkhar	10,974	2252	–	3425	19,349
Total	81,684	26,148	20,713	18,535	85,850

Table 2
Description of the ten GCMs of IPCC's Fourth Assessment Report (AR4).

Model	Abbreviation	Developer	Resolution	References
HadCm3	HADCM3	UKMO (UK)	2.5°×3.75°	Gordon et al. (2000)
ECHAM5-OM	MPEH5	MPI-M (Germany)	1.9°×1.9°	Roeckner et al. (1996)
CSIRO-MK3.0	CSMK3	ABM (Australia)	1.9°×1.9°	Gordon et al. (2002)
GFDL-CM2.1	GFCM21	NOAA/GFDL (USA)	2.0°×2.5°	Delworth et al. (2006)
MRI-CGCM2.3.2	MRCGCM	MRI (Japan)	2.8°×2.8°	K-1 model developer (2004)
CCSM3	NCCCSM	NCAR (USA)	1.4°×1.4°	Collins et al. (2006)
CNRM-CM3	CNCM3	CNRM (France)	1.9°×1.9°	Deque et al. (1994)
MIROC3.2	MIMR	NIES (Japan)	2.81°×2.81°	Hasumi and Emori (2004)
IPSL-CM4	IPCM4	IPSL (France)	2.5°×3.75°	Marti et al. (2005)
GISS-E-R	GIER	NASA/GISS (USA)	4°×5°	Schmidt et al. (2006)

makers in the study area, the study focuses on the 'near future' and has been selected. In recent decades the Zayandeh-Rud River Basin has experienced frequent water shortages. Therefore, a better picture of the near future can improve decision makers' immediate management policies.

3.2. Probability assessment

There are high levels of uncertainty in outputs of GCMs. These uncertainties affect the confidence in the results of impact assessment studies. There are many methods for dealing with such uncertainties, including but not limited to expression of the results as a central prediction, a central prediction with error bars, a known probability distribution function, a bounded range with no known probability distribution, and a bounded range within a larger range of unknown probabilities (OECD, 2003). Here, a bounded range with known probability distribution is used for dealing with the uncertainties of the ten GCMs. This probabilistic approach includes three steps:

Step 1 *Weighting the GCMs*: Each of the ten GCMs used in this study is weighted using Eq. (1), based on the Mean Observed Temperature–Precipitation (MOTP) method (Massah Bavani and Morid, 2005). To weight each model, this method considers the ability of that model in simulating the observed climate variables, i.e., the difference between the simulated average temperature and average precipitation in each month in the baseline period and the corresponding observed values:

$$W_{ij} = \frac{\left(1/\Delta d_{ij}\right)}{\sum_{j=1}^{10}\left(1/\Delta d_{ij}\right)} \quad (1)$$

where: W_{ij} is the weight of GCM j in month i; and Δd_{ij} is the difference between average temperature or precipitation simulated by GCM j in month i of base period and the corresponding observed value.

Step 2 *Construction of probability distribution functions (PDFs)*: In this step, PDFs of climate change variables are developed for each month. Fig. 3 indicates example monthly PDFs for temperature and precipitation. These PDFs relate monthly temperature and precipitation changes to the weight of corresponding GCMs. Ten climate change scenario samples, generated by ten GCMs, are used to construct a PDF for each month. This would help

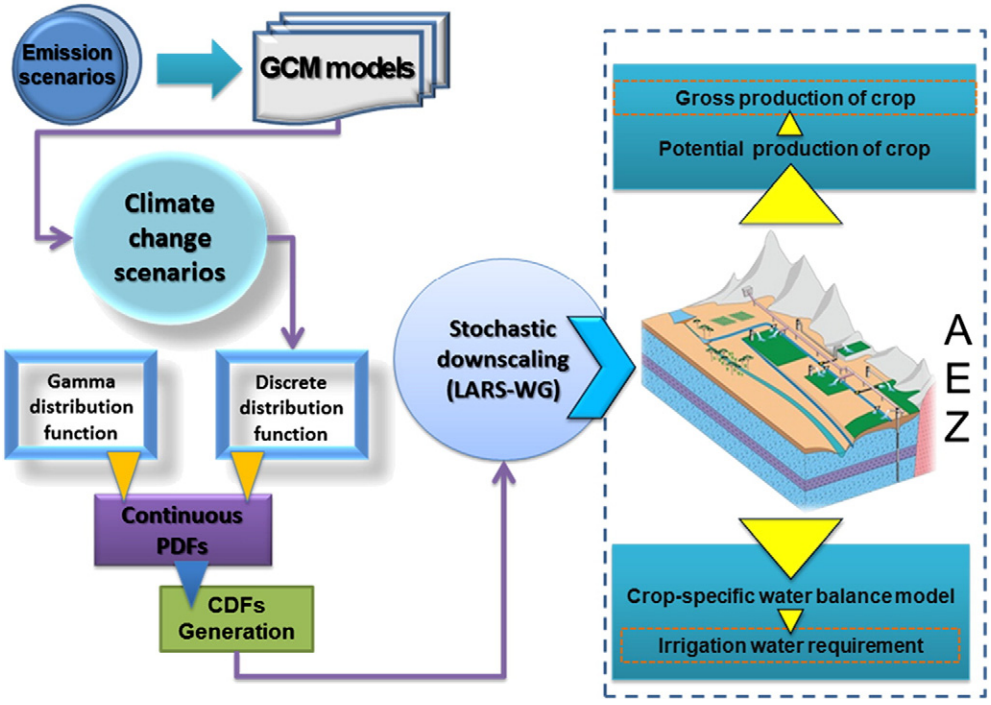

Fig. 2. Flowchart of the proposed modeling framework.

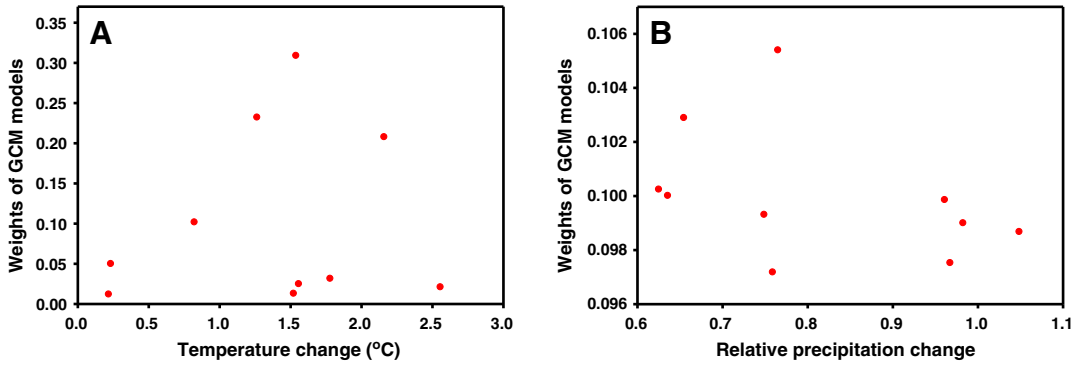

Fig. 3. Discrete PDFs, relating monthly temperature and precipitation changes to the weights of corresponding GCMs. Graph A shows the developed PDF of temperature changes in May and Graph B shows the developed PDF of relative precipitation changes in February.

converting discrete probability distributions of the main variables of climate change scenarios to continuous probability distributions. The Gamma distribution has been identified as an effective function for analyzing climatic data (Ines and Hansen, 2006; Block et al., 2009; Piani et al., 2010). Based on the prototype of discrete PDFs and similar studies (Pindyck, 2012; Teutschbein and Seibert, 2012), the Gamma distribution function with two parameters (Eq. (3)) is used to construct continuous distributions:

$$f(x) = \frac{1}{\beta^{\alpha}\Gamma(\alpha)} x^{\alpha-1} e^{-x/\beta} \quad ; x \geq 0 \tag{2}$$

where: $\bar{x}$ is the variable; α and β are shape and scale parameters for the Gamma distribution function, respectively; and $\Gamma(\alpha)$, the incomplete Gamma function, is given by Eq. (3):

$$\Gamma(\alpha) = \int_0^{\infty} x^{\alpha-1} e^{-x} dx \tag{3}$$

The values of α and β are changed to get the best fit based on the maximum likelihood estimation method. Here, the sum of squared error (Eq. (4)) is used to show how well the Gamma function fits the data:

$$\mathrm{SSE} = \sum_{i=1}^{n} (y_i - \bar{y}_i)^2 \tag{4}$$

where: y_i is the data point; $\bar{y}_i$ is the estimation of Gamma function; and n is the number of data points ($n = 10$). The small size of sample data set can affect the goodness of fit. This is indeed a limitation of this type of assessment caused by having access to a limited number of GCMs.

Step 3 *Construction of cumulative distribution functions (CDFs)*: In this step, the developed PDFs are converted to CDFs. Here, exceedance probability curves or CDFs can be developed based on the constructed PDFs from step 2 (Fig. 4). Using the developed CDFs the values of climate change variables at three different percentiles (25th, 50th, and 75th) are calculated for use as inputs to the impact assessment model later on. The 25% probability percentile represents low temperature change scenario and high precipitation change scenario where the 75% probability percentile indicates high temperature change scenario and low precipitation change scenario under climate change in the study area.

3.3. Stochastic downscaling

The outputs of GCMs are monthly changes of temperature and precipitation. Assessment of climate change impacts on agriculture should be done at finer temporal scales such as daily scales. The downscaling techniques are used to bridge the gap between the GCMs' outputs and required inputs of impacts assessment models (Wilby and Wigley, 1997). Stochastic weather generators (WG) are commonly used as downscaling tools to generate daily climate variables (Wilks and Wilby, 1985; Semenov, 2007).

LARS-WG (Semenov and Barrow, 2002) is one of the stochastic weather generators (WGs), which produces synthetic daily time series of climatic variables with any length. LARS-WG can generate daily time series from monthly climate change scenarios and historical daily climate data. As the calibration step, the WG parameters are initially calculated based on the probability distributions of locally observed daily weather variables (Semenov, 2007). This is followed by finding some semi-empirical distributions of observed data, such as

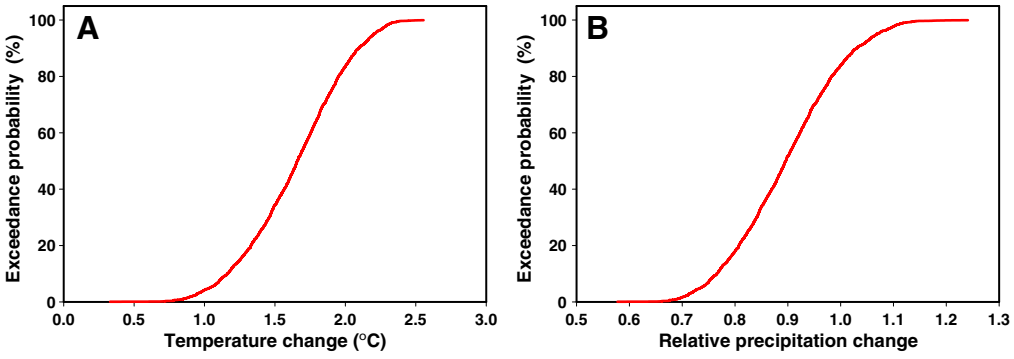

Fig. 4. Developed CDFs based on the presented PDFs in Fig. 3.

frequency distributions of the wet and dry durations. Fourier series are used for describing the precipitation amount and solar radiation, as well as minimum and maximum temperatures. In the next step, LARS-WG generates synthetic weather data using the climate change data produced earlier. In the final step, the observed data's statistical characteristics are compared with those of synthetic data. A number of statistical tests (i.e., the chi-squared test, Student's *t*-test, F-test) are used in this comparison to evaluate the differences between the distributions, and mean and standard deviation values of the synthetic and observed data sets (Semenov and Barrow, 1997; Semenov et al., 1998).

According to the objectives of this research, LARS-WG is used to generate future daily time series of maximum and minimum temperatures and precipitation under climate change scenarios. After selecting the best distribution function for the observed daily time series for baseline period (1971–200), LARS-WG generates synthetic future daily time series based on the extracted climate change scenarios for 25, 50, and 75% probability percentiles under each emission scenario. The 2015–2044 future period is selected as a near future to evaluate climate change impacts on the basin's high water demand crops. This short run assessment can help the water managers in the basin solve the ongoing and upcoming water shortage challenges.

The main drawback of using WGs is the uncertainty of climate variability. WGs produce different daily time series with equal monthly averages similar to local observed time series. The applied downscaling method in this paper tries to deal with the uncertainty in the outputs of WGs. LARS-WG is run to generate 300 years of future daily time series for each climate change probability percentile under each emission scenario. The 300-year time series is composed of 10 plausible daily time series for the 2015–2044 period. Each one of the synthetic 300-year time series is broken into 30 year daily time series and then the average daily values of the resulting 10 time series (300/30) are calculated to better deal with the uncertainty of WG in generated climatic variables.

3.4. Agro-Ecological Zones method

The Agro-Ecological Zones (AEZ) method has been developed by the Food and Agriculture Organization (FAO) and International Institute for Applied Systems Analysis (IIASA) for rational land use planning and management. This method can provide an appropriate framework for climate change assessment in crop production. Fig. 5 illustrates the flowchart of the AEZ method.

3.4.1. Crop production

3.4.1.1. Gross dry matter production of a standard crop (Y_o). Y_o is calculated using Eq. (5), based on the de Wit's concept (de Wit, 1965):

$$Y_o = F \times y_o + (1-F) \times y_c \tag{5}$$

where: Y_o is the gross dry matter production of a standard crop (kg/ha/day); R_{se} is the maximum active incoming shortwave radiation on clear days (cal/cm^2/day); R_s is the actual measured incoming shortwave radiation (cal/cm^2/day); y_o is the gross dry matter production rate of a standard crop for a given location on a completely overcast day (kg/ha/day); y_c is the gross dry matter production rate of a standard crop for a given location on a clear (cloudless) day (kg/ha/day); and F is an equation parameter, calculated using Eq. (6):

$$F = \frac{R_{se} - 0.5R_s}{0.8R_{se}}. \tag{6}$$

In this study, it is assumed that the values of R_{se}, and R_s in the future period are similar to their values in the base period.

3.4.1.2. Potential production of a standard crop (Y_{mp}). Y_{mp}, estimated based on Eq. (7), reflects the potential production of an environmentally adaptable crop under no stress and limitation:

$$Y_{mp} = C_H \times C_L \times C_N \times G \times Y_o \tag{7}$$

where: Y_{mp} is the potential production of a standard crop (kg/ha); G is the growth duration (day); C_H is the harvesting coefficient; C_L is the leaf coefficient; and C_N is the net production coefficient.

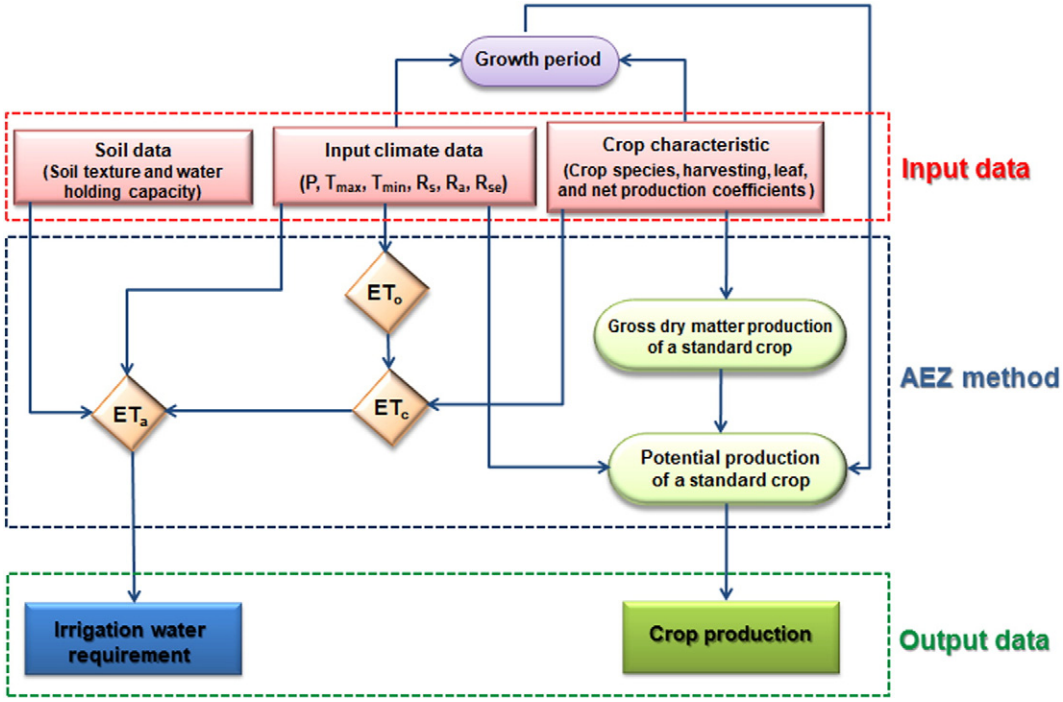

Fig. 5. Flowchart of AEZ method.

3.4.2. Crop evapotranspiration

3.4.2.1. Reference evapotranspiration (ET_o). ET_o represents the rate of evapotranspiration for 8 to 15 cm tall green grass cover of uniform height, actively growing, completely shading the ground, and not short of water (Hargreaves and Samani, 1982). There are many methods for calculating ET_o, including the Penman, Radiation, Hargreaves–Samani, and Pan Evaporation methods (Allen et al., 1996). Here, the Hargreaves–Samani's equation (Hargreaves and Samani, 1982, 1985) is used (Eq. (8)) due to having a low number of parameters, simplicity of calculations, and the desired relatively high accuracy:

$$ET_o = 0.0135 \times (K_T) \times (R_a) \times (TD)^{0.5} \times (T + 17.8) \tag{8}$$

where: T_{max} and T_{min} are maximum and minimum of daily temperature (°C) respectively; $TD = T_{max} - T_{min}$ (°C); R_a is solar radiation; T is the average daily temperature (°C); and K_T is an empirical coefficient, calculated using Eq. (9).

$$K_T = 0.00185 \times TD^2 - 0.0433 \times TD + 0.4023 \tag{9}$$

3.4.2.2. Potential crop evapotranspiration (ET_c). ET_c reflects the maximum crop water demand. ET_c increases from the planting to the flowering step (maximum value) and decreases during the maturity stage (FAO, 1998). ET_c is related to ET_o through the following relation (Eq. (10)):

$$ET_c = K_c \times Et_o \tag{10}$$

where: K_c is crop coefficient, varying during the growth period; and ET_o is the reference evapotranspiration.

3.4.3. Crop-specific water balance model

Tao et al. (2003) developed a crop-specific soil water balance model by combining FAO's (1992) crop-specified soil water balance model and Willmott et al.'s (1985) water balance model. In this model, water storage is divided into two parts: snow-cover and soil-moisture. Soil is assumed as undifferentiated layer moisture storage. The soil moisture content is calculated on a daily basis based on crop evapotranspiration, precipitation, snowmelt, and antecedent soil moisture. Water equivalent of the snow-cover (mm) at the end of day j (W_j^s) is given by Eq. (14):

$$W_j^s = W_{j-1}^s + P_j - M_j \tag{14}$$

where: W_{j-1}^s is the snow-cover water equivalent at the end of previous day $(j-1)$; and P_j is the cumulative precipitation during day j (mm). P_j may be in the form of snowfall (P_j^s) or rainfall (P_j^r), depending on T_j as dictated by Eq. (15):

$$P_j = \begin{cases} P_j^r & \text{if } T_j \geq -1\,^\circ\text{C} \\ P_j^s & \text{if } T_j \leq -1\,^\circ\text{C} \end{cases}. \tag{15}$$

As some precipitation is dropped on canopy rather than soil, it is assumed that effective precipitation is equal to 90% of actual precipitation (FAO, 1979).

Daily snowmelt (mm) in day j (M_j) is calculated using Eq. (16):

$$M_j = 2.63 + 2.55T_j + 0.0912T_jP_j^r \tag{16}$$

where: M_j is constrained, such that $0 \leq M_j \leq (W_{j-1}^s + P_j^s)$ (Storr, 1978; Willmott et al., 1985).

Soil moisture at the end of day j (W_j^c) is calculated based on Eq. (17):

$$W_j^s = \min\left(W_{j-1}^s + P_j + M_j - ET_{a\,j}, W^*\right) \tag{17}$$

where: W_{j-1}^s is the soil moisture (mm) at the end of the previous day $(j-1)$; ET_{aj} is the actual evapotranspiration (mm) in day j; and W^* is the soil's water holding capacity (mm).

The actual evapotranspiration is calculated, based on Eq. (18):

$$ET_{a\,j} = \begin{pmatrix} ET_{c\,j} & \text{if } \rho_j \geq 1 \\ \rho_j \times ET_{c\,j} & \text{if } \rho_j \text{b} 1 \end{pmatrix} \tag{18}$$

where: ρ_j, calculated using Eq. (19), represents the actual evapotranspiration proportionality factor (mm/mm):

$$\rho_j = \frac{ET_{a\,j}}{ET_{c\,j}} = \frac{W_j^s + P_j + M_j}{S_\alpha \times d \times \left(1 - P_j^c\right)} \tag{19}$$

where: S_α represents soil water holding capacity (mm/m); d represents rooting depth (m); and P_j^c represents the soil water-depletion fraction below which $ET_{aj} < ET_{cj}$.

3.4.3.1. Irrigation water requirement. Based on Fischer et al. (2001) the irrigation water requirement is the amount of added water to available soil moisture storage, which allows the crop to grow without water stress. Thus, the net irrigation water requirement for the crop growth period is calculated using Eq. (20):

$$IWR = \sum_{l=1}^{N} \sum_{k=1}^{m} \left(ET_{c\,k}^i - ET_{a\,k}^i\right)_j \tag{20}$$

where: N is the number of crops in region i and m is the number of growth days, respectively; and ET_a and ET_c are the actual and potential evapotranspiration (mm), respectively. The volume of net irrigation water requirement (WRQ) (lit) in the region i is calculated using Eq. (21):

$$WRQ_i = 10 \times IWR_i \times A_i \tag{21}$$

where A_i is the area of the irrigated lands in region i (ha).

The gross irrigation water requirement (GWR_i) (lit) is calculated through dividing WRQ_i by the irrigation efficiency parameter in region i ($Irref_i$) (Eq. (22)):

$$GWR_i = {}^{WRQ_i}\Big/_{Irref_i} \tag{22}$$

3.4.4. Growth period

The crop development depends upon air temperature in the absence of any environmental stress such as moisture and radiation. Growth degree day (GDD) is a measure of heat accumulation and can be used to predict number of days it takes for a crop to reach maturity. GDD_i is defined as the number of days that air temperature is above a certain threshold temperature. The threshold temperature is the temperature below which the crop growth is zero (Womach, 2005). The GDD_i can be calculated based on Eq. (23):

$$GDD_i = \frac{T_{\max}^i + T_{\min}^i}{2} - T_{base\,j} \tag{23}$$

where: T_{max}^i and T_{min}^i are the maximum and minimum daily temperatures (°C) in region i, respectively; and $T_{base\,j}$ is the threshold temperature for crop j, which varies by crops.

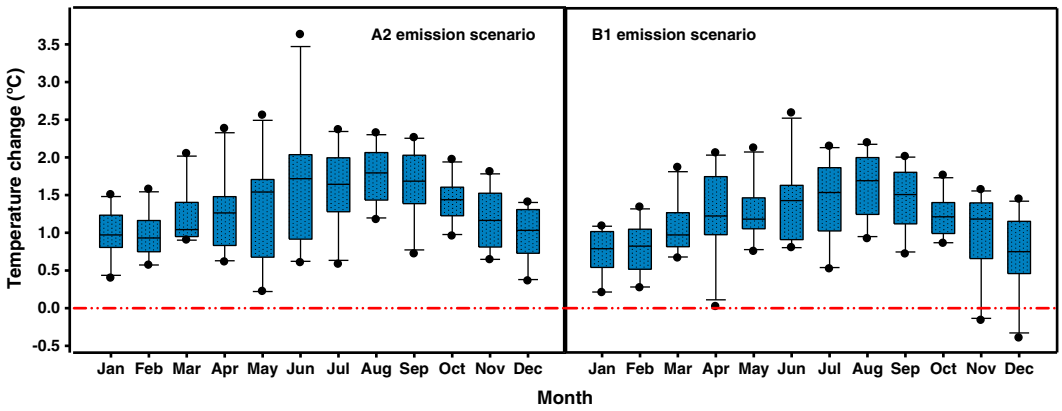

Fig. 6. Box plots (the boxes show the upper and lower quartiles, the line within shows the median, the upper and lower whiskers show the mean ± standard deviation (SD) and black circles are outliers) of the monthly change in mean temperature (°C) under different climate change scenarios. The horizontal dash–dot line in this figure illustrates no temperature change level.

3.5. Indices

To evaluate the climate change impacts on agriculture and crop production, the study benefits from different indices.

3.5.1. Crop yield ratio

Generally, the crop yield ratio (*CYR*), calculated using Eq. (24), reflects the climate change impact on potential crop yield:

$$CYR_{ij} = {}^{Y_{mpF_{ij}}}\Big/_{Y_{mpO_{ij}}} \tag{24}$$

where: $Y_{mpF_{ij}}$ and $Y_{mpO_{ij}}$ are the maximum potential yields of crop j in region i in the future and baseline periods, respectively.

3.5.2. Irrigation water requirement index

The irrigation water requirement (*IWR*) index, calculated using Eq. (25), reflects the impact of climate change on irrigation water requirement:

$$IWR_{ij} = {}^{GWR_{Fij}}\Big/_{GWR_{Oij}} \tag{25}$$

where: GWR_{Fij} and GWR_{Oij} are the gross irrigation water requirements of crop j in region i in the future and baseline periods, respectively.

3.5.3. Water productivity index

The water productivity (*WP*) index of crop j is defined as the volume of water taken by that crop to yield one unit (kg or ton) at its maximum production capacity (Eq. (26)):

$$WP_{ij} = {}^{Y_{mp\,ij}}\Big/_{ET_{av\,ij}} \tag{26}$$

where: $ET_{av\,ij}$ is volume of consumed water for crop j in region i, calculated using Eq. (27):

$$ET_{av\,ij} = \left(\sum_{j=1}^{n} ET_{a\,j}^{i}\right) \times A_i \tag{27}$$

4. Results

4.1. Regional climate change scenarios for temperature and precipitation

Figs. 6 and 7 indicate the changes in monthly temperature and precipitation, projected by ten GCM models under A2 and B1 emission scenarios for the future period (2015–2044) relative to the baseline period (1971–2000). Mean monthly temperature changes are generally expected to increase under climate change. Most GCMs suggest higher future temperatures in the study region while the range of expected temperature changes varies between scenarios. The amounts of monthly temperature changes under the A2 emission scenario are generally

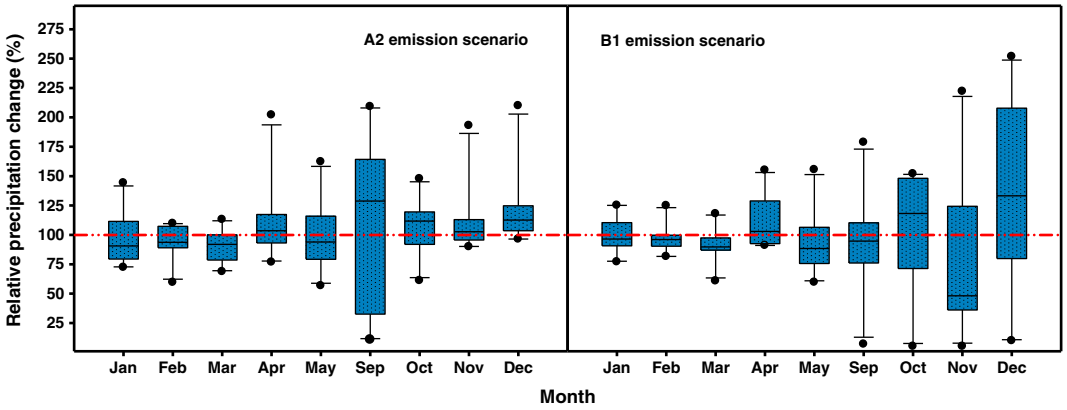

Fig. 7. Box plots (the boxes show the upper and lower quartiles, the line within shows the median, the upper and lower whiskers show the mean ± standard deviation (SD) and black circles are outliers) of the monthly relative change in mean precipitation (%) under different climate change scenarios. This figure does not include the months of June, July, and August for which the baseline precipitation was minimal. The horizontal dash–dot line shows the no precipitation change level.

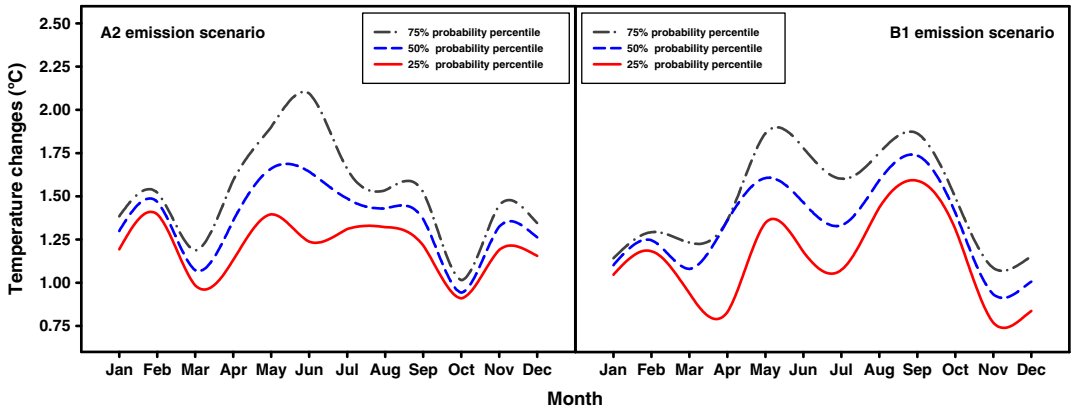

Fig. 8. Future expected temperature changes under different probability percentiles.

greater than the changes under the B1 emission scenario for all GCMs. The maximum and minimum expected temperature increase is 3.64 °C in June and −0.28 °C in December, respectively. The maximum and minimum ranges for temperature changes are expected in June and October, respectively.

Fig. 7 suggests wide ranges of precipitation changes. However, precipitation is projected to decrease in all months except February. According to Fig. 7, the maximum and minimum ranges for precipitation changes are expected in winter and fall, respectively.

The various interquartile ranges (lengths of the boxes) of different months under A2 and B1 emission scenarios reflect the uncertainty in the GCMs' output. Generally, the expected relative precipitation changes are more uncertain than the expected temperature changes. In order to manage these uncertainties, after weighting the GCMs outputs, the PDFs and CDFs of temperature and precipitation changes were developed, based on the approach explained earlier. This was followed by finding the level of expected changes in the climate change variables at three different probability percentiles (25%, 50% and 75%) using the synthetic CDFs (Figs. 7 and 8).

According to Fig. 8 temperature is expected to increase under climate change in all months at different probability percentiles and emission scenarios, but the expected level of monthly increases are very different. The values of winter and summer temperature increases under the A2 emission scenario are higher than the corresponding values under the B1 emission scenario. In contrast, simulated fall temperatures under B1 emission scenario are warmer than under the A2 emission scenario.

The expected monthly precipitation changes under climate change with respect to the baseline are very different for different probability percentiles (Fig. 9). Results suggest negative changes for some months of the year and positive changes in other months at different probability percentiles. In most cases winter precipitations are expected to decrease with climate change.

4.2. Probability distribution functions (PDFs)

The discrete PDFs of climate change scenarios were developed for each month. The parameter estimation method was used to convert the discrete PDFs to continuous ones. Tables 3 and 4 show the values of SSE and Gamma distribution parameters for continuous temperature and precipitation, respectively. The low values of SSE underline the suitability of Gamma distribution.

4.3. Downscaling the temperature and precipitation data

The expected monthly minimum and maximum temperatures and total precipitation under climate change at the three different probability percentiles were downscaled by LARS-WG to generate the local-scale daily time series of these variables according to the observed daily weather, after calibrating (Site Analysis) and validating (QTest) the model. Statistical tests were performed to assess the ability of LARS-WG to reproduce climate variability reasonably. Some statistical tests such as X^2 and t-tests were performed in QTest to determine if statistically-significant differences exist between the simulated and observed data. The small values of X^2 and t indicate that the synthetic data are very close to the observed data. Both of the tests (X^2 and t) calculate p-values, which indicate the likelihood of having similar distributions for the generated and observed data. If p-values are very low and below a selected significance level, then the generated climate is not considered to be similar to the 'true' climate

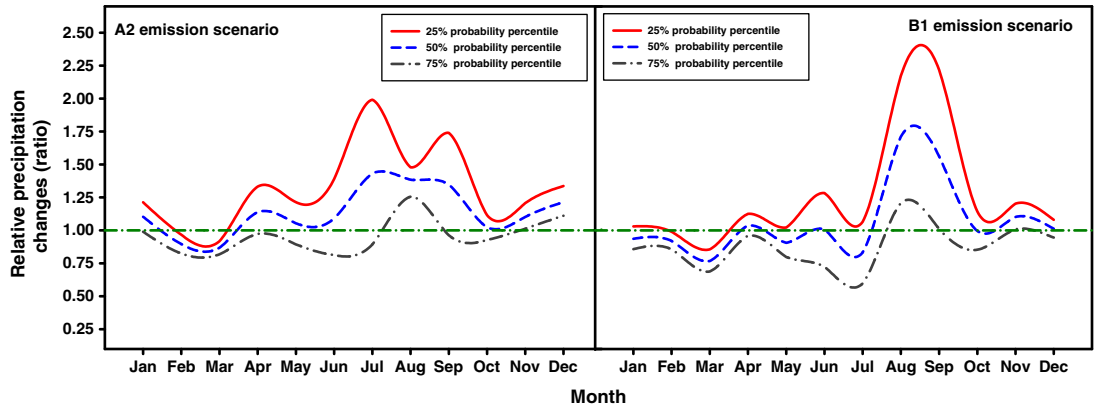

Fig. 9. Future expected relative precipitation changes under different probability percentiles. The horizontal dash–dot line shows the no precipitation change level.

Table 3
Estimated Gamma distribution parameters for temperature changes.

Emission scenario	A2					B1				
Month	SSE	α	B	a	b	SSE	α	β	a	b
Jan	0.076	9.29	2.76	0.37	1.55	0.104	16.16	1.35	0.18	1.27
Feb	0.022	12.36	1.53	0.54	1.65	0.019	15.57	1.35	0.24	1.36
Mar	0.022	1.59	7.93	0.88	2.21	0.033	2.80	5.00	0.64	1.95
Apr	0.019	3.00	4.00	0.59	2.44	0.035	3.95	4.00	0.00	2.21
May	0.074	6.00	4.00	0.19	2.65	0.047	3.00	3.35	0.73	2.15
Jun	0.064	2.00	3.81	0.58	3.83	0.069	2.05	3.35	0.78	2.88
July	0.066	6.42	6.39	0.55	2.38	0.087	2.75	3.78	0.57	2.17
Aug	0.125	5.85	6.28	1.15	2.35	0.101	5.19	6.65	0.91	7.42
Sep	0.135	5.02	6.89	0.70	2.30	0.136	7.95	3.85	0.70	7.26
Oct	0.044	0.57	6.28	0.90	2.19	0.129	7.06	5.07	0.84	1.81
Nov	0.069	6.00	4.50	0.67	1.85	0.020	8.41	5.19	−0.18	1.66
Dec	0.106	9.00	2.50	0.30	1.54	0.095	9.28	3.50	−0.42	1.54

*a and b are minimum and maximum temperature change values for each PDFs. These parameters indicate the domain of temperature changes for each month.

Table 4
Estimated Gamma distribution parameters for precipitation changes.

Emission scenario	A2					B1				
Month	SSE	α	β	a*	b*	SSE	α	β	a*	b*
Jan	0.013	3.00	3.00	0.78	1.56	0.019	2.40	7.72	0.72	1.72
Feb	0.027	5.81	6.80	0.55	1.37	0.014	3.46	7.26	0.71	1.45
Mar	0.035	5.027	6.69	0.65	1.16	0.019	3.40	7.65	0.52	1.46
Apr	0.023	2.00	5.50	0.72	2.42	0.023	2.83	7.45	0.83	1.72
May	0.021	3.00	3.50	0.51	1.74	0.022	4.07	7.71	0.52	1.71
Jun	0.095	2.40	4.00	0.28	2.51	0.062	3.00	3.00	0	2.01
July	0.074	1.50	1.90	0.15	3.11	0.059	3.00	3.15	0	1.72
Aug	0.192	10.00	2.00	0	1.62	0.020	2.50	1.99	0	3.25
Sep	0.108	3.00	4.00	0.05	3.15	0.106	2.58	8.86	0	7.45
Oct	0.025	6.75	6.22	0.53	1.52	0.027	2.00	2.50	0.61	1.54
Nov	0.021	2.50	7.77	0.85	1.95	0.027	2.83	4.50	0.82	1.67
Dec	0.055	2.20	6.50	0.94	2.15	0.034	5.44	6.73	0.75	1.44

*a and b are minimum and maximum precipitation change values for each PDFs. These parameters indicate the domain of precipitation changes for each month.

(Semenov and Barrow, 2002). The results of these statistical tests for minimum and maximum temperatures and precipitation are shown in Table 5. Here, the significance level was set to 0.05 (commonly used in statistical tests). Given that the p-values of the three variables are higher than the selected significance level in all months of year, the generated daily time series are considered to be satisfactory.

Figs. 10 and 11, respectively, show the estimated local (downscaled) temperature and precipitation for all months of year under climate change for various probability percentiles. In general, temperature increases are expected under all climate change scenarios in all months. But, the levels of increase vary between months. The ranges of temperature changes are larger under B1 emission scenario than under the A2 scenario due to more rapid global socioeconomic and population growth in the near future period. The maximum temperature changes are expected in spring months. Unlike the results for temperature, the local precipitation changes do not show a general increasing trend. Similar to the temperature changes, the ranges of precipitation changes under B1 emission scenario are larger than the changes under the A2 emission scenario. The results show that the maximum monthly precipitation will decrease in winter.

The projected annual and seasonal changes of 30-year mean temperature and total precipitation were calculated under different probability percentiles of climate change (Table 6). With 11–31% decrease in precipitation and 1.1–1.5 °C increase in temperature at annual scale, the basin will face warmer and drier conditions under climate change. The maximum seasonal changes are predicted for winter precipitation (24–41% reduction) and spring temperature (1.86 °C increase).

4.4. Climate change impacts on agriculture

4.4.1. Impacts on growth period

The estimated growth period changes are shown in Fig. 12. The growth periods of all crops are projected to get shorter with climate change due to the raising growth period temperature in absence of irrigation water shortage. Table 7 reports relative temperature changes in the growth period for the four considered crops. The maximum growth period shortenings are expected to be 24 days for barley and 20 days for wheat. The growth periods of rice and corn are expected to get shortened by 2 to 3 days and 2 to 4 days, respectively, which are significantly lower than the expected growth period changes for wheat and barley. Depending on the local climatic condition, shortening of the growth period has the potential for more economic benefits though providing more time to the farmers for land preparation and an opportunity for cultivation of alternative crops with short growth periods before cultivation of the main crop (alternative cultivation).

4.4.2. Impacts on crop production

An important purpose of this study was to evaluate the crop production in the Zayandeh-Rud River Basin under climate change. It is noteworthy that here we are not considering the climate change impacts on irrigation water availability in the basin, assuming that crop water demand can be fully satisfied through surface water and groundwater sources of the basin. This, indeed, enables us to estimate the climate change (temperature and precipitation changes) effects on potential crop production under no water tension, leading to estimation of the additional water requirement for crop irrigation under climate change. However, with this approach we cannot estimate the actual crop production of the basin under climate change. Future

Table 5
The statistical details of LARS-WG verification.

Month	Precipitation				Minimum temperature				Maximum temperature			
	X^2	p-Value	t	p-Value	X^2	p-Value	t	p-Value	X^2	p-Value	t	p-Value
Jan	0.27	0.63	−0.79	0.43	0.10	0.999	−0.36	0.71	0.10	0.999	−0.96	0.54
Feb	0.08	1.00	−0.41	0.68	0.05	1.000	−0.37	0.70	0.11	0.998	0.94	0.55
Mar	0.06	1.00	−0.30	0.77	0.05	1.000	−1.65	0.77	0.05	1.000	−0.22	0.62
Apr	0.08	1.00	1.48	0.14	0.05	1.000	0.13	0.89	0.05	1.000	−0.46	0.64
May	0.07	1.00	−0.74	0.46	0.05	1.000	0.51	0.60	0.05	1.000	−0.21	0.83
Jun	0.12	0.99	−0.29	0.78	0.11	0.998	1.03	0.46	0.11	0.998	0.82	0.72
Jul	0.26	0.36	0.55	0.58	0.11	0.998	1.19	0.83	0.11	0.998	1.21	0.31
Aug	0.33	0.13	−0.49	0.62	0.11	0.998	−0.64	0.61	0.11	0.998	1.29	0.37
Sep	0.07	1.00	0.23	0.82	0.10	0.999	−1.86	0.58	0.05	1.000	−1.41	0.62
Oct	0.30	0.19	0.55	0.98	0.05	1.00	−1.94	0.66	0.05	1.000	0.17	0.98
Nov	0.10	1.00	1.40	0.17	0.05	1.00	−0.69	0.23	0.05	1.000	−0.79	0.43
Dec	0.09	1.00	1.23	0.22	0.10	0.998	1.12	0.30	0.11	0.998	0.33	0.85

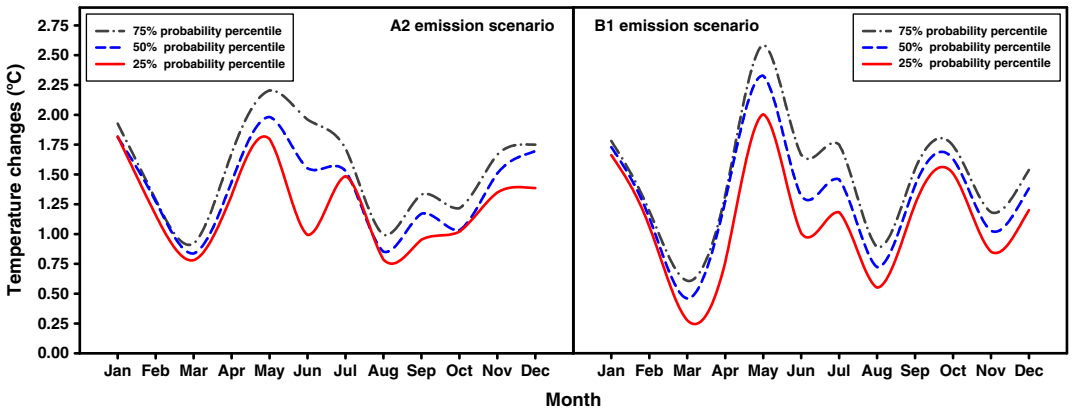

Fig. 10. The local temperature change under climate change at different probability percentiles.

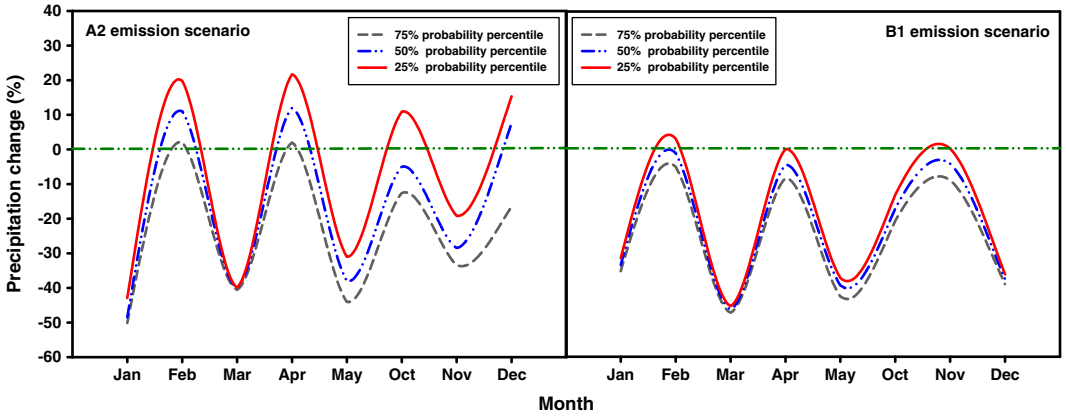

Fig. 11. The local precipitation change under climate change for different probability percentiles (This figure does not include the four months of June, July, August and September, due to the minimal baseline precipitation levels). The horizontal dash–dot line shows the no precipitation change level.

studies may consider the climate change impacts on water availability in the basin to estimate the crop yield of the basin under climate change.

As discussed earlier the *CYR* is used to study the crop yield changes under climate change. Fig. 13 shows the estimated *CYR* of the four important crops of the study area under different emission scenarios at different probability percentiles. While the *CYR* values change by crop types and emission scenarios all values are less than 1, reflecting the negative climate change impact on production of wheat, barley, rice and corn in the Zayandeh-Rud River Basin. Based on Fig. 13 and Table 7, the decrease in CYR is correlated with the decrease in growth period temperature. Therefore, decrease in growth period temperature is the major driver for decreasing crop production under the no water tension assumption. The ranges of production changes are −2.5 to −20.7%, −1.4 to −17.2%, −2.1 to −9.5% and −5.7 to −19.1% for wheat, barley, rice and corn, respectively.

The findings of this study about crop production changes are consistent with those of the similar recent studies in other regions. For example, You et al. (2009) reported that rising temperature over the past two decades has led to a 4.5% decline in wheat production in China. Chaves et al. (2009) studied potential climate change impacts on the production of major crops (corn, potato, rice, and winter wheat) of eastern China. Their results indicated that potential production declines by 2.5 to 12% for all studied cases due to the expected increase in temperature, which will reduce the growth period (Alexandrov and Hoogenboom, 2000). In another study Ozdogan (2011) estimated

Table 6
Annual and seasonal changes in climatic variable under different probability percentiles.

Scenario		A2-25%	A2-50%	A2-75%	B1-25%	B1-50%	B1-75%	Maximum	Minimum
Temperature change (°C)	Annual	1.2	1.36	1.52	1.13	1.32	1.47	1.52	1.13
	Fall	1.08	1.18	1.27	0.97	1.12	1.24	1.27	0.97
	Winter	1.19	1.28	1.36	1.06	1.14	1.22	1.36	1.06
	Spring	1.26	1.55	1.86	1.12	1.48	1.67	1.86	1.12
	Summer	1.28	1.43	1.57	1.37	1.55	1.74	1.74	1.28
Precipitation change (%)	Annual	−10.66	−17.29	−25.44	−31.01	−23.87	−16.47	−31.01	−10.66
	Fall	3.86	−5.44	−21.37	−12.79	−20.26	−27.97	−27.97	3.86
	Winter	−23.94	−28.11	−31.36	−29.36	−35.51	−41.11	−41.11	−23.94
	Spring	3.02	−5.71	−14.33	11.43	0.96	−9.17	−14.33	11.43
	Summer	−100.0	−100.0	−100.0	−100.0	−100.0	−100.0	−100.0	−100.0

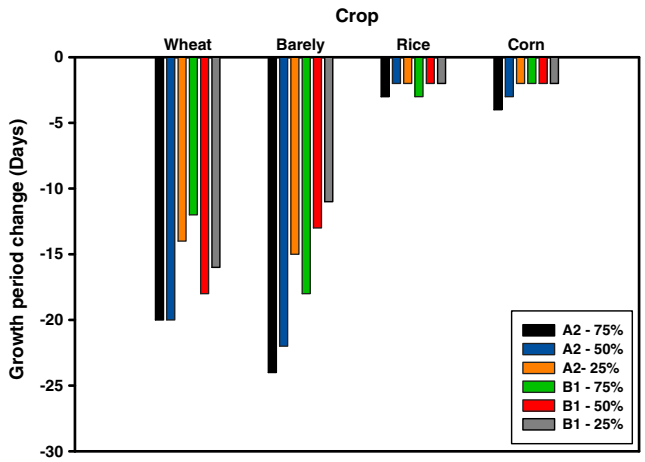

Fig. 12. Crop growth period changes under different emission scenarios and probability percentiles.

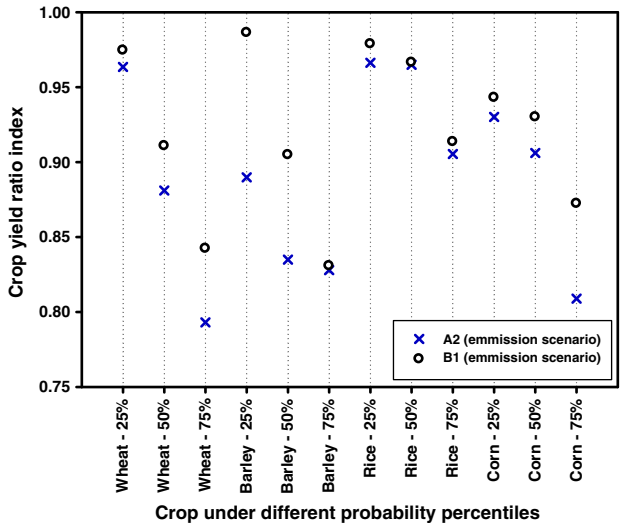

Fig. 13. Crop yield ratio (*CYR*) under different probability percentiles for different crops.

a decrease of 5 to 35% in winter wheat productions in northwestern Turkey under the future warmer and drier conditions.

4.4.3. Impact on irrigation water requirements

As discussed earlier, IWR index is considered in this study to evaluate climate change impacts on irrigation water requirements (Fig. 14). The estimated IWR index suggests that irrigation water requirements increase for all crops with climate change. The maximum values of irrigation water requirement changes are 30.2% and 24.9% for rice and corn, respectively. According to Table 7, the growth period temperature changes of rice and corn are higher than those of wheat and barley. Therefore, irrigation water requirement changes for rice and corn are more than the changes for wheat and barley due to higher evapotranspiration under higher temperatures. This is consistent with the findings of some other climate change studies. For example, Tao and Zhang (2010) estimated an increase of 15.6–21.8% in irrigation water requirements under climate change in North China Plain. In another study, Guo et al. (2010) suggested an increase in irrigation water requirement of wheat by 3–19% in north China due to warming effects on evapotranspiration under climate change.

4.4.4. Impacts on water productivity

Fig. 15 indicates the estimated of WP index for different probability percentiles and emission scenarios. According to this figure, WP index of all crops decrease with climate change. The estimated WP index changes of wheat, barley, rice and corn are between −18.3 to 0.5%, −16.7 to 12.9, −23.2% to −10.4% and −18.2 to −4.2%, respectively. Lower crop WP is projected with higher growth period temperature. This is due to the increased evapotranspiration with climate warming. Similar finding was obtained by Guo et al. (2010) who estimated that WP index of wheat and corn change by −8.1 to 4.3% and −36.1 to −2.0% with climate change.

Table 7
Temperature changes (°C) in the growth period under different emission scenarios and probability percentiles.

	Wheat	Barley	Rice	Corn
A2 75%	1.40	1.25	1.64	1.56
A2 50%	1.05	0.93	1.35	1.32
A2 25%	0.92	0.56	1.05	0.97
B1 75%	1.65	1.88	1.80	1.64
B1 50%	1.06	0.95	1.42	1.40
B1 25%	0.62	0.63	1.29	1.23

5. Limitations

While the study approach provides valuable insights into the studied problem, the modeling method is associated with some limitations, which need to be considered when interpreting the results. In specific, the study has three major limitations that may be addressed by future studies. First, due to access to a limited number of GCMs, the proposed modeling framework produces the probability distribution of climate change variables using ten GCMs. The small size of sample data set ($n = 10$) can affect the goodness of fit when developing probability distribution functions. Second limitation relates to the assumption of no irrigation water shortage in projection of crop production under climate change. This assumption is based on the fact that availability of water for irrigation is also affected by water rights and the management policies in the basin. However, climate change might reduce the water availability in the basin, which can in turn affect crop production. Therefore, this study takes an optimistic approach and perhaps overestimates crop production under climate change. Third, as the first study of climate change impacts on crop production in the Zayandeh-Rud River Basin, this study only focuses on simulating the impacts under the business-as-usual scenario,

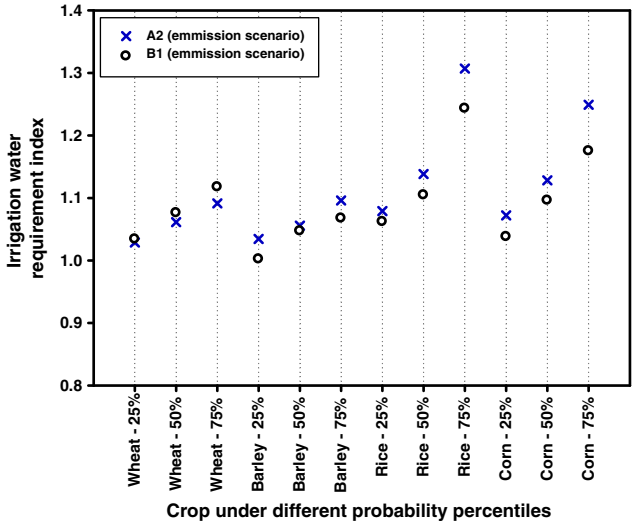

Fig. 14. Irrigation water requirement index (*IWR*) under different emission scenarios and probability percentiles.

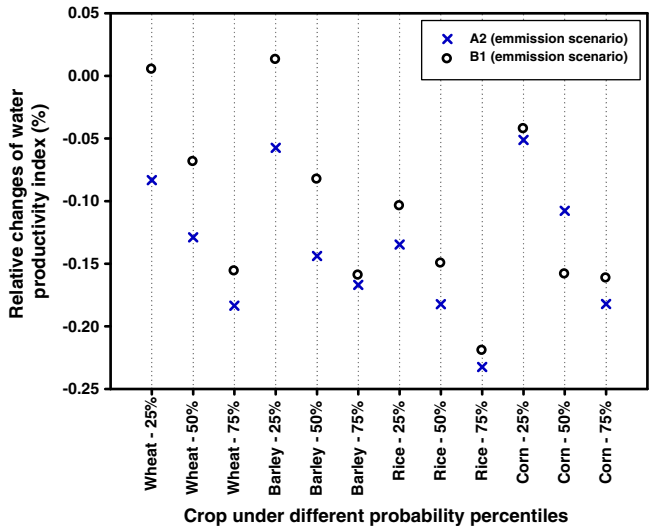

Fig. 15. Water productivity (*WP*) index under different emission scenarios and probability percentiles.

i.e. management policies (water allocation to the agricultural sector, crop types, area under cultivation, etc.) remain the same. However, cropping patterns can be affected by water availability, urbanization, technological improvements, and the economic conditions of the region in the future. Also, climate change effects can be mitigated to some extent though implementing appropriate adaptation measures. Future studies of climate change impacts on crop productivity in the study area could consider the socio-economic changes in the basin as well as the possibility of changing in the water management structure and policies in the study area to adapt to future conditions.

6. Conclusions

In this study ten GCMs are used to estimate climate change impacts on agriculture in the Zayandeh-Rud River Basin under two emission scenarios. To deal with the high uncertainty in the estimated temperature and precipitation changes under climate change, a weighted ensemble of GCMs' outputs was generated and climate change variables at three different risk levels (25%, 50%, and 75%) were estimated. Downscaled climate variables suggest that generally temperature will rise in the study area while the level of temperature increase varies between months (with the maximum increase expected in spring). Monthly precipitation changes do not show a general increasing or decreasing trend. Nevertheless, the maximum monthly precipitation reduction (11–31%) will occur in winter and annual precipitation is expected to decrease by 10.7 to 31%. This can be of considerable importance for the Zayandeh-Rud River Basin with semi-arid Mediterranean climate in which winter precipitation is the main source of renewable water supply.

Estimated impacts of climate change on agriculture in the basin suggest that in a dry warm future crop production will decrease significantly (2.5% to 20.7% for wheat, 1.4% to 17.2% for barley, 2.1% to 9.5% for rice, and 5.7% to 19.1% for corn). Due to temperature increases, crop irrigation water requirements will increase under climate change. However, growing period is shortened with warming under no water limitation (i.e., when irrigation water is not reduced and farmers are allowed to replace surface water with groundwater).

As a result of decreased crop production and increased irrigation water requirements, the water productivity (WP) of all crops will decrease under dry climate warming. This means that crop yield would reduce even if the same amount of irrigation water were available. The minimum values of future WP are expected for rice and corn, with significantly higher water requirements than wheat and barley. Therefore, continued cultivation of these locally high value crops cannot be justified under climate change, which can have significant economic effects in the Zayandeh-Rud River Basin. The obtained results about non-suitability of rice for cultivation in the study area comply with the findings of Morid and Massah Bavani (2010). Given that water is the major limitation to agriculture in arid and semi-arid regions, climate change adaptation policies in the basin should include changing crop type as well as water productivity and irrigation efficiency enhancement at farm and regional scales.

Acknowledgment

This paper was written during the first author's stay at the University of Central Florida (UCF) as a visiting scholar. This author would like to thank Iran's Ministry of Science, Research and Technology (MSRT) and Isfahan University of Technology, for financial support during his stay at UCF. Special thanks go to the Hydro-Environmental and Energy Systems Analysis (HEESA) Research Group at UCF for hospitality and their extensive support during this research. The authors thank the three anonymous reviewers for their constructive and thoughtful comments.

References

Abrishamchi A, Jamali S, Madani K, Hadian S. Climate change and hydropower in Iran's Karkheh River Basin. Proceeding of the 2012 World Environmental and Water Resources (EWRI) Congress, ASCE; 2012 May 20–25. Albuquerque, New Mexico, USA: ASCE; 2012. p. 3341–9.

Alexandrov VA, Hoogenboom G. The impact of climate variability and change on crop yield in Bulgaria. Agric For Meteorol 2000;104:315–27.

Allen RG, Periera LS, Raes D, Smith M. Crop evapotranspiration. FAO irrigation and drainage paper no. 56. Rome: FAO; 1996.

Bader DC, Covey C, Gutowski WJ, Held IM, Kunkel KE, Miller RL. Climate models: an assessment of strengths and limitations. U.S. climate change science program synthesis and assessment product 3.1. Washington DC: Department of Energy, Office of Biological and Environmental Research; 2008 [124 pp.].

Block PJ, Souza Filho FA, Sun L, Kwon HH. A stream flow forecasting framework using multiple climate and hydrological models 1. J Am Water Resour Assoc 2009;45(4): 828–43.

Brian A, Joyce BA, Mehta VK, Purkey DR, Dale LL, Hanemann M. Modifying agricultural water management to adapt to climate change in California's central valley. Clim Chang 2011;109:299–316.

Buytaert W, Celleri R, Timbe L. Predicting climate change impacts on water resources in the tropical Andes: effects of GCM uncertainty. Geophys Res Lett 2009;36:L07406. http://dx.doi.org/10.1029/2008GL037048.

Cai X, Wang D, Laurent R. Impact of soil moisture under climate change on crop yield—a case study of rain fed corn in central Illinois. J Appl Meteorol 2009a;48:1868–81.

Cai X, Wang D, Zhu T, Ringler C. Assessing the regional variability of GCM simulations. Geophys Res Lett 2009b;36:L02706. http://dx.doi.org/10.1029/2008GL036443.

Chaves DR, Izaurralde RC, Thomson AM, Gao X. Long-term climate change impacts on agricultural productivity in eastern China. Agric For Meteorol 2009;149:1118–28.

Chen C, Wang EYuQ. Modelling the effects of climate variability and water management on crop water productivity and water balance in the North China Plain. Agric Water Manag 2010;97:1175–84.

Collins WD, Bitz CM, Blackmon ML, Bonan GB, Bretherton CS, Carton JA, et al. The community climate system model: CCSM3. J Clim 2006;19:2122–43.

Connell-Buck CR, Medellín-Azuara J, Lund JR Madani K. Adapting California's water system to warm vs. dry climates. Clim Chang 2011;109(Suppl. 1):133–49.

Connolley WM, Bracegirdle TJ. An antarctic assessment of IPCC AR4 coupled models. Geophys Res Lett 2007;34:L22505. http://dx.doi.org/10.1029/ 2007gl031648.

Daccache A, Weatherhead EK, Stalham MA, Knox JW. Impacts of climate change on irrigated potato production in a humid climate. Agric For Meteorol 2011;151: 1641–53.

de Wit CT. Photosynthesis of leaf canopies. Agric Res report 1965;63:57. [Reports 663, Wageningen, Netherland: Pudoc].

Delworth TL, Broccoli AJ, Rosati A, Stouffer RJ, Balaji V, Beesley JA. GFDL's CM2 global coupled climate models, part I: formulation and simulation characteristics. J Clim 2006;19:643–74.

Deque M, Dreveton C, Braun A, Cariolle D. The ARPEGE/Ifs atmosphere model: a contribution to French community climate modeling. Clim Dyn 1994;10:249–66.

Elmahdi A, El-Gafy I, Kheireldin K. WBFS model: strategic water and food security planning on national wide level. IGU-2008 Water sustainability commission: Tunis; 2008.

Eslamian SS, Gilroy KL, McCuen RH. Climate change detection and modeling in hydrology. Climate change—research and technology for adaptation and mitigation. In Tech; 2012. p. 87-100.

FAO. Report on the agro-ecological zones project: methodology and results for Africa. World soil resources report 48. Rome: FAO press; 1978.

FAO. Report on yield response to water. FAO irrig. and drain. paper no. 33. Rome: FAO press; 1979.

FAO. CROPWAT: a computer program for irrigation planning and management. FAO irrigation and drainage paper 46. Rome: FAO press; 1992.
FAO. Report on crop evapotranspiration. Irrigation and drainage paper No. 56. FAO publicationRome: FAO press; 1998.
Fischer G, Tubiello FN, van Velthuizen H, Wiberg DA. Climate change impacts on irrigation water requirements: effects of mitigation, 1990–2080. Technol Forecast Soc Chang 2001;74:1083–107.
Furrer RR, Knutti R, Sain SR, Nychka DW, Meehl GA. Spatial patterns of probabilistic temperature change projections from a multivariate Bayesian analysis. Geophys Res Lett 2007;34:L06711. http://dx.doi.org/10.1029/2006GL027754.
Gordon C, Cooper C, Senior CA, Banks H, Gregory JM, Johns TC, et al. The simulation of SST, sea ice extents and ocean heat transports in a version of Hadley Center coupled model without flux adjustments. Clim Dyn 2000;16:147–68.
Gordon HB, Rotstayn LD, McGregor JL, Dix MR, Kowalczyk EA, O'Farrell SP, et al. The CSIRO Mk3 climate system model (electronic publication). CSIRO Atmospheric Research technical paper no. 60. Aspendale: CSIRO Atmospheric Research; 2002. [Available online at http://www.dar.csiro.au/publications/gordon_2002a.pdf].
Greene AM, Goddard L, Lall L. Probabilistic multi-model regional temperature change projections. J Clim 2006;19:4326–46.
Guegan M, Uvo CB, Madani K. Developing a module for estimating climate warming effects on hydropower pricing in California. Energy Policy 2012;42:261–71.
Guo R, Lin Z, Mo X, Yang C. Responses of crop yield and water use efficiency to climate change in the North China Plain. Agric Water Manag 2010;97:1185–94.
Hargreaves GH, Samani ZA. Estimating potential evapotranspiration. J Irrig Drain E-ASCE 1982;108:223–30.
Hargreaves GH, Samani ZA. Reference crop evapotranspiration from temperature. Trans ASABE 1985;1:96–9.
Hasumi H, Emori S. K-1 coupled model (MIROC) description, K-1 technical report no. 1. University of Tokyo: Center for Climate System Research; 2004.
Hoglind M, Thorsen SM, Semenov MA. Assessing uncertainties in impact of climate change on grass production in North Europe using ensembles of global climate models. Agric For Meteorol in press; http://dx.doi.org/10.1016/j.agrformet.2012.02.010.
Ines AVM, Hansen JW. Bias correction of daily GCM rainfall for crop simulation studies. Agric For Meteorol 2006;138(1–4):44–53.
IPCC. General guidelines on the use of scenario data for climate impact and adaptation assessment. Cambridge and New York: Cambridge University Press; 2007.
Jonesa PG, Thornton PK. The potential impacts of climate change on maize production in Africa and Latin America in 2055. Global Environ Chang 2003;13:51–9.
K-1 model developer. K-1 coupled model (MIROC) description. K-1 technical report No. 1. Center for Climate System Research, University of Tokyo; 2004.
Kloster S, Dentener F, Feichter J, Raes F, Lohmann U, Roeckner E, et al. A GCM study of future climate response to aerosol pollution reductions. Clim Dyn 2010;34:1177–94.
Knutti R, Abramowitz G, Collins M, Eyring V, Gleckler PJ, Hewitson B, et al. Good practice guidance paper on assessing and combining multi model climate projections. Meeting report of the intergovernmental panel on climate change expert meeting on assessing and combining multi model climate projections. Bern, Switzerland: IPCC Working Group I Technical Support Unit, University of Bern; 2010.
Laux P, Jackel G, Tingem RM, Kunstmann H. Impact of climate change on agricultural productivity under rainfed conditions in Cameroon—a method to improve attainable crop yields by planting date adaptations. Agric For Meteorol 2010;150:1258–71.
Lee J, Gryze SD, Six J. Effect of climate change on field crop production in California's Central Valley. Clim Chang 2011;109:335–53.
Liu S, Mo X, Lin Z, Xu Y, Ji J, Wen G, et al. Crop yield responses to climate change in the Huang-Huai-Hai Plain of China. Agric For Meteorol 2010;97:1195–209.
Lizumi T, Yokozawa M, Nishimori M. Parameter estimation and uncertainty analysis of a large-scale crop model for paddy rice: application of a Bayesian approach. Agric For Meteorol 2009;149:333–48.
Lobell DB, Field CB. California perennial crops in a changing climate. Clim Chang 2011;109:317–33.
Lopez A, Tebaldi C, New M, Stainforth DA, Allen MR, Kettleborough JA. Two approaches to quantifying uncertainty in global temperature changes. J Clim 2006;19:4785–96.
Madani K, Lund JR. Estimated impacts of climate warming on California's high-elevation hydropower. Clim Chang 2010;102:521–38.
Madani K, Marino MA. System dynamics analysis for managing Iran's Zayandeh-Rud River Basin. Water Resour Manag 2009;23:2163–87.
Marti O, Braconnot P, Bellier J, Benshila R, Bony S, Brockmann P, et al. The new IPSL climate system model: IPSL-CM4. Technical report. Paris: Institute Pierre Simon Laplace des Sciences de l'Environment Global; 2005.
Massah Bavani AR, Morid S. The impacts of climate change on water resources and agricultural production. J Water Resour Res 2005;1:40–7. [(In Persian)].
Masutomi Y, Takahashi K, Matsuoka Y. Impact assessment of climate change on rice production in Asia in comprehensive consideration of process/parameter uncertainty in general circulation models. Agr Ecosyst Environ 2009;131:281–91.
Medellin-Azuara J, Harou JJ, Olivares MA, Madani K, Lund JR, Howitt RE, et al. Adaptability and adaptations of California's water supply system to dry climate warming. Clim Chang 2008;87:75–90.
Mo X, Liu S, Lin Z, Guo R. Regional crop yield, water consumption and water use efficiency and their responses to climate change in the North China Plain. Agr Ecosyst Environ 2009;134:67–78.
Morid S, Massah Bavani AR. Exploration of potential adaptation strategies to climate change in the Zayandeh Rud irrigation system, Iran. J Irrig Drain E-ASCE 2010;59:226–38.
Moss RH, Schneider SH. Uncertainties in the IPCC TAR: recommendations to lead authors for more consistent assessment and reporting. Guidance papers on the cross cutting issues of the third assessment report of the IPCC. Geneva: World Meteorological Organization; 2000. p. 33–51.
Mozny M, Tolasz R, Nekovar J, Sparks T, Trnka M, Zalud Z. The impact of climate change on the yield and quality of Saaz hops in the Czech Republic. Agric For Meteorol 2009;149:913–9.
Murphy JM, Booth BBB, Collins M, Harris GR, Sexton DMH, Webb MJ. A methodology for probabilistic predictions of regional climate change from perturbed physics ensembles. Phil Trans R Soc A 2007;365:1993–2028.
Niu X, Easterling W, Hays CJ, Jacobs A, Mearns L. Reliability and input-data induced uncertainty of the EPIC model to estimate climate change impact on sorghum yields in the U.S. Great Plains. Agr Ecosyst Environ 2009;129:268–76.
OECD. Special Issue on Climate Change: Climate Change Policies: Recent development and long term issues. Paris: Organization for Economic Cooperation and Development (OECD) publications; 2003.
O'Neal MR, Nearing MA, Vining RC, Southworth J, Pfeifer RA. Climate change impacts on soil erosion in Midwest United States with changes in crop management. Catena 2005;61:165–84.
Ozdogan M. Modeling the impacts of climate change on wheat yields in northwestern Turkey. Agr Ecosyst Environ 2011;141:1-12.
Parry ML, Rosenzweig C, Iglesias A, Livermore M, Fischer G. Effects of climate change on global food production under SRES emissions and socio-economic scenarios. Global Environ Chang 2004;14:53–67.
Piani C, Haerter JO, Coppola E. Statistical bias correction for daily precipitation in regional climate models over Europe. Theor Appl Climatol 2010;99(1):187–92.
Pindyck RS. Uncertain outcomes and climate change policy. J Environ Econ Manag 2012;63(3):289–303.
Roeckner E, Oberhuber JM, Bacher A, Christoph M, Kirchner I. Enso variability and atmospheric response in a global coupled atmospheric-ocean GCM. Clim Dyn 1996;12:737–54.
Roudier P, Sultan B, Quirion P, Berg A. The impact of future climate change on West African crop yields: what does the recent literature say? Global Environ Chang 2011;21:1073–83.
Sajjad Khan M, Coulibaly P, Dibike Y. Uncertainty analysis of statistical downscaling methods. J Hydrol 2006;319:357–82.
Schlenker W, Lobell DB. Robust negative impacts of climate change on African agriculture. Environ Res Lett 2010;5:1–8.
Schmidt GA, Ruedy R, Hansen JE, Aleinov I, Bell N, Bauer M, et al. Present day atmospheric simulations using GISS ModelE: comparison to in-situ, satellite and reanalysis data. J Clim 2006;19:153–92.
Schmittner A, Latif M, Schneider B. Model projections of the North Atlantic thermohaline circulation for the 21st century assessed by observations. Geophys Res Lett 2005;32:L23710.
Semenov MA. Development of high-resolution UKCIP02-based climate change scenarios in the UK. Agric For Meteorol 2007;144:127–38.
Semenov MA, Barrow EM. Use of a stochastic weather generator in the development of climate change scenarios. Clim Chang 1997;35:397–414.
Semenov MA, Barrow EM. LARS-WG: a stochastic weather generator for use in climate impact studies. Version 3.0 user manual; 2002.
Semenov MA, Brooks RJ, Barrow EM, Richardson CW. Comparison of the WGEN and LARS-WG stochastic weather generators for diverse climates. Clim Res 1998;10:95-107.
Storr D. A comparison of daily snowmelt calculated by the US crops of engineers theoretical model with measured amounts on a snow pillow. Storm Water Resources Consulting Service. British, Columbia: Ganges; 1978.
Tao F, Zhang Z. Adaptation of maize production to climate change in North China Plain: quantify the relative contributions of adaptation options. Eur J Agron 2010;33:103–16.
Tao F, Zhang Z. Climate change, wheat productivity and water use in the North China Plain: a new super-ensemble based probabilistic projection. Agric For Meteorol in press; http://dx.doi.org/10.1016/j.agrformet.2011.09.002.
Tao F, Yokozawa M, Hayashi Y, Lin E. Changes in agricultural water demands and soil moisture in China over the last half-century and their effects on agricultural production. Agric For Meteorol 2003;118:251–61.
Tao F, Yokozawa M, Zhang Z. Modeling the impacts of weather and climate variability on crop productivity over a large area: a new process-based model development, optimization, and uncertainties analysis. Agric For Meteorol 2009;149:831–50.
Teixeira EI, Fischer G, van Velthuizen H, Walter C, Ewert F. Global hot-spots of heat stress on agricultural crops due to climate change. Agric For Meteorol in press; http://dx.doi.org/10.1016/j.agrformet.2011.09.002.
Teutschbein C, Seibert J. Bias correction of regional climate model simulations for hydrological climate-change impact studies: review and evaluation of different methods. J Hydrol 2012;456–457:12–29.
Thomson AM, Izaurralde RC, Rosenberg NJ, He X. Climate change impacts on agriculture and soil carbon sequestration potential in the Huang-Hai Plain of China. Agr Ecosyst Environ 2006;114:195–209.
Waugh DW, Eyring V. Quantitative performance metrics for stratospheric resolving chemistry-climate models. Atmos Chem Phys 2008;8:5699–713.
White JW, Hoogenboom G, Kimball BA, Wall GW. Methodologies for simulating impacts of climate change on crop production. Field Crop Res 2011;124:357–68.
Wilby RL, Harris I. A framework for assessing uncertainties in climate change impacts: low-flow scenarios for the River Thames, UK. Water Resour Res 2006;42:W02419. http://dx.doi.org/10.1029/2005WR004065.
Wilby RL, Wigley TML. Downscaling general circulation model output: a review of methods and limitations. Prog Phys Geogr 1997;21:530–48.
Wilks DS, Wilby RL. The weather generation game: a review of stochastic weather models. Prog Phys Geogr 1985;23:329–57.
Willmott CJ, Rowe CN, Mintze Y. Climatology of the terrestrial seasonal water cycle. J Climatol 1985;5:589–606.
Womach J. Agriculture: a glossary of terms, programs and laws. In: Congressional research service report, editor. CRS-132; 2005.

Xu C-Y, Gong L, Jiang T, Chen D, Singh VP. Analysis of spatial distribution and temporal trend of reference evapotranspiration in Changjiang (Yangtze River) Catchment. J Hydrol 2006;327:81–93.
You L, Rosegrant MW, Wood S, Sun D. Impact of growing season temperature on wheat productivity in China. Agric For Meteorol 2009;149:1009–14.
Zayandab Consulting Engineering Co. Determination of resources and consumptions of water in the Zayandeh-Rud River Basin, Iran; 2008.
Zhang XC, Liu WZ. Simulating potential response of hydrology, soil erosion, and crop productivity to climate change in Changwu tableland region on the Loess Plateau of China. Agric For Meteorol 2005;131:127–42.
Zhang XC, Nearing MA. Impact of climate change on soil erosion, runoff, and wheat productivity in central Oklahoma. Catena 2005;61:185–95.
Zhang Q, Xu C-Y, Zhang Z, Chen YD, Liu C-L. Spatial and temporal variability of precipitation maxima during 1960–2005 in the Yangtze River basin and possible association with large-scale circulation. J Hydrol 2008;353:215–27.
Zhang Q, Xu C-Y, Tao H, Jiang T, Chen YD. Climate changes and their impacts on water resources in the arid regions: a case study of the Tarim River basin, China. Stoch Environ Res Risk Assess 2010;24:349–58.
Zhu Q, Jiang H, Peng C, Liu J, Wei X, Fang X. Evaluating the effects of future climate change and elevated CO_2 on the water use efficiency in terrestrial ecosystems of China. Ecol Model 2011;222:2414–29.